Science of the Total Environment 586 (2017) 197–205

Contents lists available at ScienceDirect

Science of the Total Environment

journal homepage: www.elsevier.com/locate/scitotenv

Assessment of 21st century drought conditions at Shasta Dam based on dynamically projected water supply conditions by a regional climate model coupled with a physically-based hydrology model

T. Trinh [a,*], K. Ishida [a], M.L. Kavvas [a], A. Ercan [b], K. Carr [b]

[a] Hydrologic Research Laboratory, Dept. of Civil and Environmental Engineering, Univ. of California, Davis, CA, United States
[b] J. Amorocho Hydraulics Laboratory, Dept. of Civil and Environmental Engineering, Univ. of California, Davis, CA, United States

HIGHLIGHTS

- This manuscript considers 13 future projections based on 4 scenarios to characterize droughts at Shasta Dam Watershed.
- The proposed approach uses a hydro-climate model (WEHY-HCM) to generate equally likely 13 future water supply projections.
- The future water supply were compared to the current water demand for the estimation of drought properties.
- The results suggest an increasing water scarcity at Shasta Dam with more severe and longer future drought events.

GRAPHICAL ABSTRACT

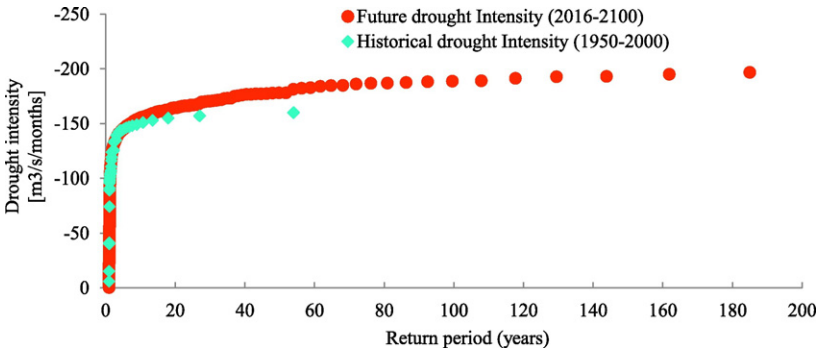

ARTICLE INFO

Article history:
Received 17 October 2016
Received in revised form 29 January 2017
Accepted 29 January 2017
Available online 3 February 2017

Editor: D. Barcelo

Keywords:
Global climate model (GCM)
Watershed Environmental Hydrology Hydro-Climate Model (WEHY-HCM)
Shasta Dam watershed (SDW),emission scenarios
Drought condition
Climate projections

ABSTRACT

Along with socioeconomic developments, and population increase, natural disasters around the world have recently increased the awareness of harmful impacts they cause. Among natural disasters, drought is of great interest to scientists due to the extraordinary diversity of their severity and duration. Motivated by the development of a potential approach to investigate future possible droughts in a probabilistic framework based on climate change projections, a methodology to consider thirteen future climate projections based on four emission scenarios to characterize droughts is presented. The proposed approach uses a regional climate model coupled with a physically-based hydrology model (Watershed Environmental Hydrology Hydro-Climate Model; WEHY-HCM) to generate thirteen equally likely future water supply projections. The water supply projections were compared to the current water demand for the detection of drought events and estimation of drought properties. The procedure was applied to Shasta Dam watershed to analyze drought conditions at the watershed outlet, Shasta Dam. The results suggest an increasing water scarcity at Shasta Dam with more severe and longer future drought events in some future scenarios. An important advantage of the proposed approach to the probabilistic analysis of future droughts is that it provides the drought properties of the 100-year and 200-year return periods without resorting to any extrapolation of the frequency curve.

* Corresponding author.
E-mail addresses: tqtrinh@ucdavis.edu (T. Trinh), kishida@ucdavis.edu (K. Ishida), mlkavvas@ucdavis.edu (M.L. Kavvas), aercan@ucdavis.edu (A. Ercan), kjcarr@ucdavis.edu (K. Carr).

http://dx.doi.org/10.1016/j.scitotenv.2017.01.202
0048-9697/

1. Introduction

Drought has been considered as the most complex natural phenomenon related to a shortage of some kind. Occurrence of a drought may cause disruption in water supply to natural environment, as well as to agricultural, municipal, and other activities of a society (Pereira et al., 2002). Definitions of drought vary with duration and severity of the phenomenon, water sources and uses, and drought's effects on human activities. The American Meteorological Society (1997) completed a thorough review of drought definitions, which can be classified into four overall categories: meteorological, agricultural, hydrological and socioeconomic droughts. The meteorological drought is expressed as a prolonged and abnormal precipitation deficiency. The agricultural drought is related to deficit in soil moisture to satisfy the requirements of a particular crop at a particular time. The hydrologic drought is related to deficiencies in surface and subsurface water supplies. Last but not the least, the socioeconomic drought occurs when the water demand exceeds the supply and impairs social and economic crises. Meanwhile, the socioeconomic drought is considered as the combination of meteorological, agricultural and hydrological droughts in term of many sectors of the economy.

Obtaining drought properties is the first step in planning water resources in order to prevent and mitigate the negative impacts of future drought occurrences (Vogel, 1987). Knowing that impacts of drought are gradual and may last for many years, the reliable drought analyses require high quality primary data that satisfy the following conditions: (i) the data should be long enough to be trustworthy in a statistical sense, (ii) the data should consistently capture dry and wet events, (iii) the data should cover the whole study area uniformly, and (iv) the data should be easily accessible (Rossi et al., 2007). Since global reanalysis datasets and other global climate model (GCM) simulated data generally satisfy these conditions, these global datasets have been applied to drought studies in many parts of the world. Dirmeyer and Brubaker (1999) used the National Centers for Environmental Prediction (NCEP) reanalysis dataset (Kalnay et al., 1996) at 6 hourly intervals to examine drought conditions during the spring and summer of 1988 over the United States. Bonaccorso et al. (2003) identified the spatial variability of drought conditions over the region of Sicily, Italy using the NCEP reanalysis dataset from 1948 to 1996. Xin et al. (2006) analyzed the meteorological drought based on the 40-yr reanalysis data of the European Centre for Medium-Range Weather Forecasts (ERA-40) (Uppala et al., 2005) during 1958–2000 over the south of the Yangtze River. Ohara et al. (2011) assessed the water balance of the Tigris-Euphrates River Basin covering four countries including Turkey, Syria, Iraq, and Iran, based on NCEP reanalysis dataset.

In dealing with projections of future drought conditions at local scales, studies usually use projections from GCMs which represent climate change conditions in the future (Cayan et al., 2010; Cook, 2008; Kirono et al., 2011; Madadgar and Moradkhani, 2011; Prudhomme et al., 2014). It is acknowledged that such global data typically divide the globe up into grid squares whose resolutions are often on the range of 150–600 km (Flato et al., 2013; Trinh et al., 2016a; Xu, 1999). Projection outputs coming directly from the global data are clearly insufficient for detailed analyses of regional water resources conditions (Adam et al., 2009; Ohara et al., 2010). Downscaling techniques are therefore needed to transform these coarse resolution global data to the finer resolution data to be used in local scales. There are two primary types of downscaling used, dynamical and statistical. Similar to GCMs, the dynamical downscaling uses the numerical atmospheric modeling to represent the physical climate processes, but is applied at much finer scales over study areas (Trinh et al., 2016a). The statistical downscaling technique generally uses statistical relationships derived between observed local climate data and the global outputs data, and applies them to simulate climate data cover the whole study domain (Anderson et al., 2007; Jang and Kavvas, 2013). The dynamical downscaling is much more demanding in terms of computational resources, but it has the advantage of being able to uniformly cover a region regardless of the location of observing stations (Anderson et al., 2007; Jang and Kavvas, 2013). While the statistical downscaling is less demanding, it is dependent on observations data available in both time and space (Milly et al., 2007). After completing a downscaling process, some studies analyzed the meteorological drought conditions based on downscaled precipitation, and temperature (Dutra et al., 2013; Ghosh and Mujumdar, 2007; Raziei et al., 2011), some others transferred these downscaled atmospheric variables to streamflow data for hydrologic, agricultural, and socioeconomic drought analyses (Mishra et al., 2010; Sheffield et al., 2004).

A critical issue in drought studies is detection of drought events and properties. Drought events in any category are first identified by appropriate indexes, and then their properties are characterized by statistical techniques. Through the years, a variety of indexes have been developed to evaluate the water deficits including: Palmer drought severity index (PDSI) (Palmer, 1965), crop moisture index (CMI) (Palmer, 1968), surface water supply index (SWSI) (Shafer and Dezman, 1982), soil moisture drought index (SMDI) (Hollinger et al., 1993), standardized precipitation index (SPI) (McKee et al., 1995; McKee et al., 1993), aggregated drought index (Keyantash and Dracup, 2004), streamflow drought index (SDI) (Nalbantis, 2008), and standardized runoff index (SRI) (Shukla and Wood, 2008). However, few indexes take into account the water demand which is required to assess the reliability of the drought analysis by comparing it with water supply.

In this study, an objective evaluation of future drought conditions at a watershed was performed. For an objective evaluation, future water supply was compared with the current water demand conditions. Then water deficits and surpluses at the watershed under future conditions were estimated from this comparison. The watershed of Shasta Dam in Northern California, which will be referred to as the Shasta Dam watershed (SDW), was selected as the study region. The water supply and water demand at Shasta Dam are considered to be the water supply and water demand at the target watershed in this study. Future water supply was projected based on dynamical downscaling of climate change scenarios into streamflows using the Hydro-Climate Model WEHY-HCM. Previously, Trinh et al. (2016b) implemented the WEHY-HCM over the SDW, and validated the model by comparing historical downscaled precipitation, simulated snowfall and snowmelt, and streamflow data with the corresponding historical observations over the SDW. After the validation, they reconstructed those valuables for a 50-year historical period (1950–2000). In this study the WEHY-HCM with the validated configuration in the previous study will be used to project atmospheric, snowfall and snowmelt, and stream flow conditions from 2016 to 2100, and evaluate future drought conditions at the target watershed.

The results of this study are based on given projected greenhouse gas emission scenarios in order to plan Shasta Dam"s future water resources within the framework of climate change, and to provide information on the impacts of future potential climate change on the water resources of the specified region. Such information is expected to be especially helpful for water managers to deal with the future planning of water budgets in Shasta Dam watershed. This study is expected to contribute a new approach to the study of future droughts in a specified region.

2. Study area

The Shasta Dam watershed (SDW) is located in Northern California and Southcentral Oregon, and is a sub-watershed of the Sacramento River watershed (Fig. 1). SDW is located among three major mountain ranges: Sierra-Nevada Mountain range in the east, Cascade Range in the north, and Klamath Mountains in the west. The watershed consists approximately of 18,907 km^2 land area that is primarily covered by forest land and shrub, with elevations ranging from 308 m to 4206 m. The geological condition of the watershed is defined by the geomorphic features of the Klamath Mountains and the Cascade region. Rock units of

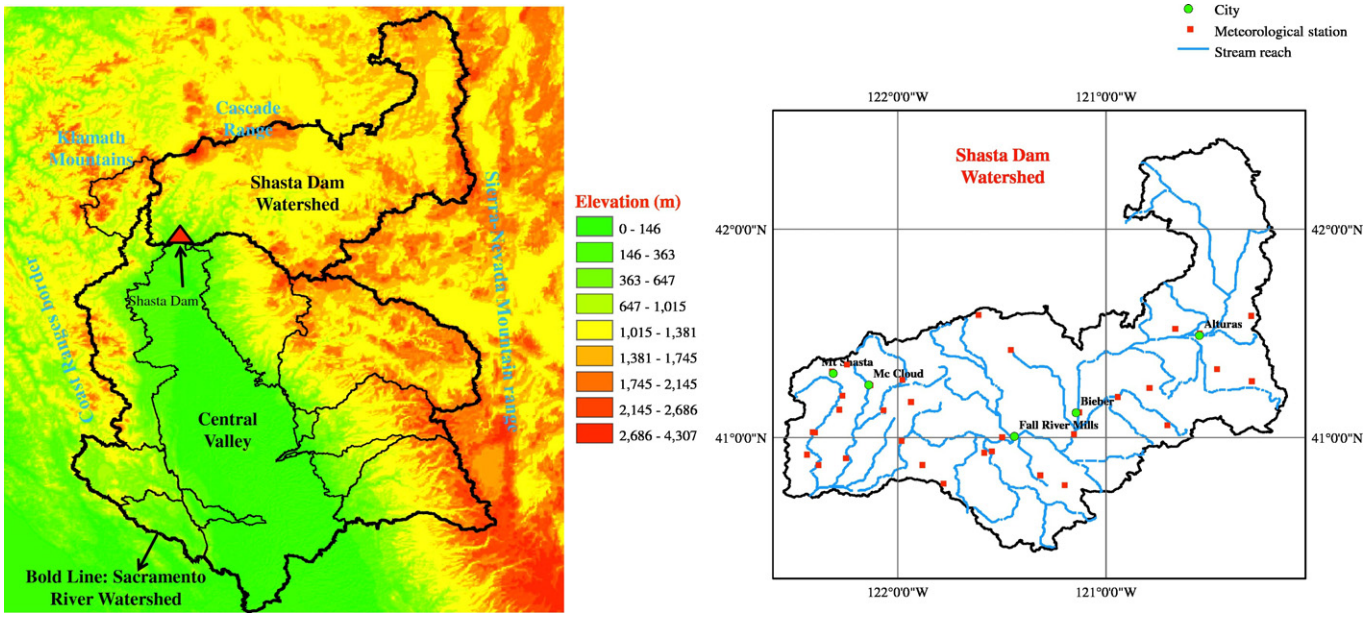

Fig. 1. Plan view of the Shasta Dam watershed in California.

the Klamath Mountains are mainly metasedimentary with iron-rich ultramafics and silica-rich granitics, thus castle crags are a unique geologic feature in this region (DWR, 2013). The Cascade region is characterized by rhyolitic to basaltic volcanic activity (DWR, 2013). Many characteristic volcanic features can be found in the region such as glass (obsidian) flows, lava flows, pumice deposits, lava tubes, cinder cones, and craters (DWR, 2013). The region includes two main groundwater basins underlying metamorphic rocks, and volcanic-rock aquifers with an area of about 100 km^2 (DWR, 2013). Generally, groundwater quality in SDW is excellent. Due to its large area, average annual precipitation in SDW is spatially distributed in a wide range over the SDW (from 254 mm to 1778 mm per year), and the majority of annual precipitation falls mostly during the cold wet season, from November through April. The downstream end of SDW is Shasta Dam. Shasta Dam provides water mainly for agricultural farm lands in California's Central Valley project (CVP) that is one of the Nation's major water conservation developments. Although Shasta Dam is only one of 20 dams and reservoirs under CVP, it has been a keystone of the project since it provides clean, dependable water supply for municipal and industrial use, wildlife habitat maintenance, navigation through the Sacramento River and power generation that benefits millions of people miles away from the shores of Shasta Lake. Therefore, climatic variations and changes in and around SDW can have a significant effect on the water supply system of CVP, and thereby, California.

3. Methodology

In this study, a methodology for the assessment of drought conditions in a watershed for future time periods, based on the future water supply and the current water demand conditions, is proposed. Schematic description of the proposed drought analysis methodology is presented in Fig. 2. The estimation of water supply (inflow) to Shasta Dam starts by obtaining GCM future climate projections which provide three-dimensional atmospheric data of climate projections at coarse resolution (>150 km) under different emission scenarios during the 21st century. Thirteen future projections from the two GCMs based on four emission scenarios were utilized for this study. These two GCMs are the third-generation atmospheric global climate model (CCSM3) (Collins et al., 2006) and the fifth generation of the ECHAM general circulation model (ECHAM5) (Roeckner et al., 2003). Future climate projections were obtained from the two GCMs because they provide three-dimensional atmospheric data at six-hour time increments that are suitable for the dynamical downscaling by a coupled atmospheric-hydrologic model. The CCSM3 was developed by an international community of students and scientists from universities and national laboratories led by USA, and the ECHAM5 was developed at the Max Planck Institute for Meteorology. As listed in Table 1, climate projections for A1B, B1, A2, A1FI emission scenarios, under only one single initial condition, were considered from CCSM3; and A1B, A2 and B1 scenarios for three different initial conditions were considered from ECHAM5 model in order to obtain nine individual projections (A1B1, A1B2, A1B3, A2-1, A2-2, A2-3, B1-1, B1-2, B1-3). The more detailed information for CCSM3 and ECHAM5 can be found at Collins et al. (2006) and Roeckner et al. (2003).

Recognizing that the resolution of future GCM climate projections are too coarse to directly use for analyzing the water resources at watershed or regional scales (Flato et al., 2013), the coarse resolution future climate data was dynamically downscaled to finer resolution (9 km) by means of the validated WEHY-HCM atmospheric module (Trinh et al., 2016b). The downscaled climate projection data were then used to simulate snowfall and snowmelt processes by means of the validated WEHY-HCM snow module as input to WEHY-HCM hydrologic module. Stream inflows to Shasta Dam from the validated WEHY-HCM hydrologic module output were compared with the current Shasta Dam's water demand to determine the characteristics of the potential drought conditions at Shasta Dam during the 21st century. The water demand from Shasta Dam under the current conditions and regulations were obtained from a previous study by Trinh et al. (2016b). Then socioeconomic drought analyses were performed to determine the characteristics of potential drought conditions at Shasta Dam during 21st century.

3.1. Hydro-Climate Model WEHY-HCM

The Watershed Environmental Hydrology Hydro-Climate Model, WEHY-HCM, was selected to project the water supply at Shasta Dam during the 21st century. The WEHY-HCM is a coupled model of atmospheric and hydrologic processes at watershed scale, based on the WEHY watershed hydrology model that is coupled with a regional climate model. Through the atmospheric boundary layer (Kavvas et al., 2013). The WEHY model consists of a snow accumulation and snowmelt module and a watershed hydrologic module. These modules were also employed in the WEHY-HCM. Then the MM5 (The Fifth-Generation

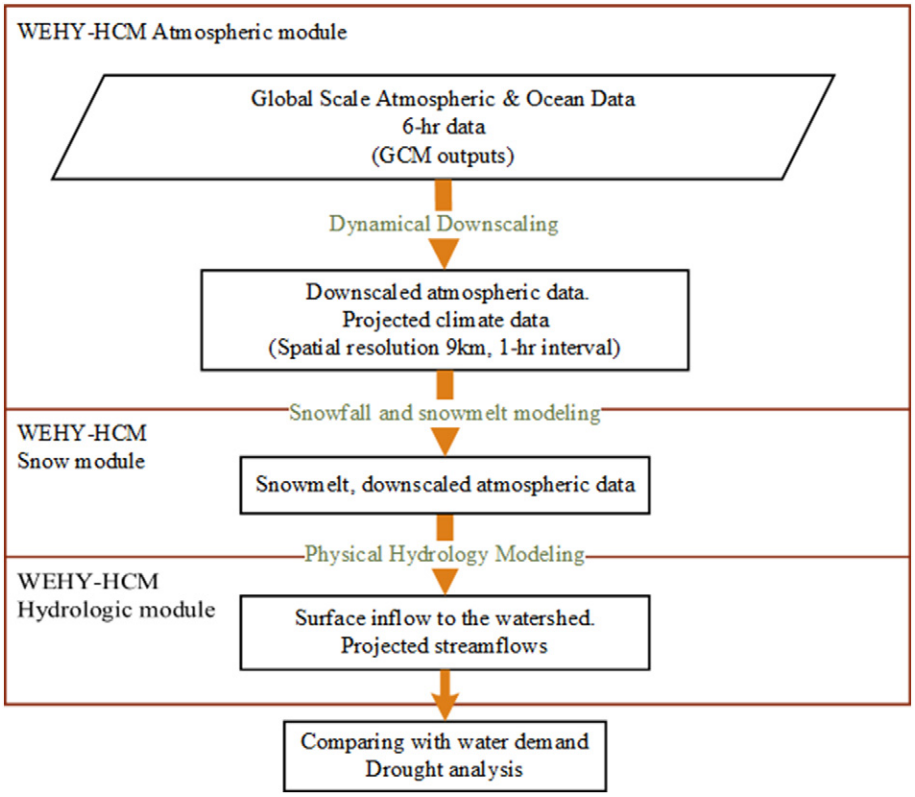

Fig. 2. Schematic description of the proposed drought analysis methodology.

PSU/NCAR mesoscale model) (Grell, 1995) atmospheric model was utilized as the regional climate model for the WEHY-HCM regional atmospheric module in this study.

The MM5 is a terrain following, sigma coordinate, non-hydrostatic model that allows multiple levels of nesting. It can dynamically downscale data to as small as a 0.5–1 km resolution, allowing it to capture the impact of steep topography and land surface/land use conditions of watersheds on the local atmospheric conditions. Physics options used in MM5 model configuration are tabulated in Table 2.

The WEHY-HCM snow and hydrologic modules were developed at the Hydrologic Research Laboratory at UC Davis. The snow module is a physically based model (energy budget model) with the assumption of linear vertical snow temperature profile in calculating the snowmelt process. The snow module is based on the depth averaged energy balance equations that were developed by Horne and Kavvas (1997), and extended by Ohara and Kavvas (2006) in order to incorporate the effect of topography-modified solar radiation on the spatial distribution of snowmelt, snow temperature, and snow depth, explicitly. The requirements snow module input include physical data such as elevation, land cover, land use, and surface slope and aspect, which are coupled with downscaled atmospheric data for the estimation of snowmelt, snow temperature, snow depth, snow density, and freezing depth which vary in time.

The hydrologic module uses upscaled conservation equations through their ensemble averaged forms in order to describe the evolution of the hydrologic processes within a watershed in time and space (Chen et al., 2004a; Chen et al., 2004b; Kavvas et al., 2004). Thereby, the WEHY-HCM hydrologic module can be considered a scalable hydrologic model. The hydrologic module upscales from all grid points over a watershed domain to the scale of the computational grid areas (model computational unit, MCU). In order to account for the surface and subsurface hillslope hydrologic processes, these MCUs are either individual hillslopes or first-order sub-watersheds within a watershed. The hydrologic module describes interception, bare soil evaporation, direct evaporation from ponded water over the plant leaves, and plant transpiration through root water uptake in dynamic interaction with the soil moisture. Such processes briefly separate hydrologic processes into five components including unsaturated flow, subsurface storm flow, overland flow, ground water flow, and channel flow, which are computed in parallel. The surface and subsurface flow components of the hydrologic module are able to simulate both the Hortonian and variable source area flow mechanisms. Although the subsurface soil root zone may not be saturated to the soil surface, Hortonian overland flow may still occur due to ponding of infiltration-excess rainfall/snowmelt water over the land surface. In some areas, such as vegetated landscapes, water from rainfall or snowmelt can infiltrate vertically down to the root zone as unsaturated flow until encountering a hardened soil layer beneath the plant roots. At this layer the soil hydraulic conductivity decreases drastically, impeding the vertical soil water flow. Over this soil impeding layer, the soil water ponds and saturates soil pores.

Table 1
The global climate models and projections used in this study.

GCM	Available projections	Horizontal grid resolution	The future simulation period
ECHAM5	9 A1B1, A1B2, A1B3, A2-1, A2-2, A2-3, B1-1, B1-2, B1-3	1.8	2016–2100
CCSM3	4 A1B, A1FI, A2, B1	1.4	2016–2100

Table 2
MM5 model configuration.

MM5 model configuration	The selected option
Cumulus parameterization	Kain-Fritsch (Kain, 2004)
Micro-physics processes	Mixed-Phase (Reisner et al., 1998)
PBL schemes	MRF (Hong and Pan, 1996)
Radiation schemes	Cloud-radiation (Dudhia, 1989)
Surface schemes	Five-layer thermal diffusion model (Dudhia, 1996)

When soil water attains "saturation state", a flow known as the "subsurface storm flow" (Dunne, 1978) moves downslope within a hillslope and continues to be replenished by vertical unsaturated flow. If the unsaturated flow in the subsurface zone continues to go down vertically through the unsaturated zone, it can reach an underlying groundwater aquifer. In this way, deep unconfined groundwater aquifers may be replenished. Subsurface flow in excess of the transmission capacity of the soil horizon returns from the subsurface to the surface and becomes overland flow. These processes are based on physical parameters obtained from geographic information system databases (topography, geomorphology, soil, and land use and land cover). Details of the hydrologic module and its parameters can be found in Chen et al. (2004a, 2004b) and Kavvas et al. (2004). Details of the implementation of the hydrologic module in the SDW can be found in Trinh et al. (2016b). Sample model parameters for SDW are presented in Fig. 3.

The regional atmospheric, snow and hydrology modules of WEHY-HCM were successfully validated at the SDW by comparing their simulated results, based on NCEP reanalysis data, with the corresponding observations during a historical period in a previous study (Trinh et al., 2016b). The downscaled precipitation data by the atmospheric module were compared with the corresponding ground observations from the Parameter-Elevation Regressions on Independent Slopes Model (PRISM) (Daly et al., 2008) during the period from 1950 to 2000 over SDW (Trinh et al., 2016b). The simulated snow water equivalent by the snow module was compared against ground observations during a 10-year period of September 30, 1999, through September 30, 2009 (Trinh et al., 2016b). The simulated surface flow was validated with 9-years-long inflow observations at Shasta Dam (October 1995 to October 2004). In general, the model-simulated hydro-climate matches the corresponding observation data well with respect to temporal and spatial distributions, thus validating the proposed model (Trinh et al., 2016b).

3.2. GCMs' validation

Although GCMs might be one of the best tools for the estimation of future climate change, the use of GCMs' simulations introduces considerable uncertainty (Dosio and Paruolo, 2011; Hawkins and Sutton, 2009; Maurer, 2007; Maurer and Duffy, 2005; Teutschbein and Seibert, 2012). Various sources of uncertainty have been recognized in future climate change studies such as GCM structure and parameter uncertainty, greenhouse gas emissions scenarios uncertainty, and GCMs initial conditions uncertainty (Hawkins and Sutton, 2009). Currently, a large number of GCMs, greenhouse gas emissions scenarios (GGES), and downscaling methods are available. It is increasingly difficult to quantify the uncertainties that result from future projections considering the combination of sources of such uncertainty. Furthermore, simplifying assumptions are unavoidable when developing these models of climate change. One recommendation to decrease uncertainty is the use of a validation process that verifies GCMs outputs (Trinh et al., 2016a). Because GCMs" simulations focus on the climatology of a specified period rather than the prediction of actual changes for the future periods, model validation using the frequency curve of the model's ensemble future climate projections is recommended. For this study, the future climate projections were validated by comparing the frequency curve of annual mean flow, simulated by the WEHY-HCM as inflow to Shasta Dam, with the one obtained from the observation inflow record, as function of the return period. An annual mean flow as function of the return period describes the probability of an annual mean flow of a certain magnitude. The WEHY-HCM parameters for the projection of future water supply were the same as those obtained from the validation processes in Trinh et al. (2016b). Since the GCMs" future projection data from the two selected GCMs existed for 2001–2100, this study used model-simulated ensemble of thirteen individual climate projections of annual mean inflow (4 from CCSM3 and 9 from ECHAM5) to Shasta Dam during 2001–2015 to compare with the observed annual inflow data taken directly from the California Data Exchange Center (CDEC) for the validation purpose. A comparison between the model-simulated and observed annual inflows for various return periods is exhibited in Fig. 4. This comparison shows that the model-simulated and observed flows matched fairly closely. The two-sample Kolmogorov-Smirnov (KS) test that was used to assess the differences between model-simulated and observed (from flow record) flow discharges for various return periods, passed at a 5% significance level, indicating the two flow frequency curves were from the same distribution, thus validating the proposed GCMs.

3.3. Identification of drought events

Once the downscaled GCM-projections-based watershed modeling approach is validated, it is important to identify drought events based on the future water supply and water demand. Shasta Dam inflow was modeled using the validated WEHY-HCM with the atmospheric initial and boundary conditions provided from GCMs' projection outputs (ECHAM5 and CCSM3). Such model simulation information can be

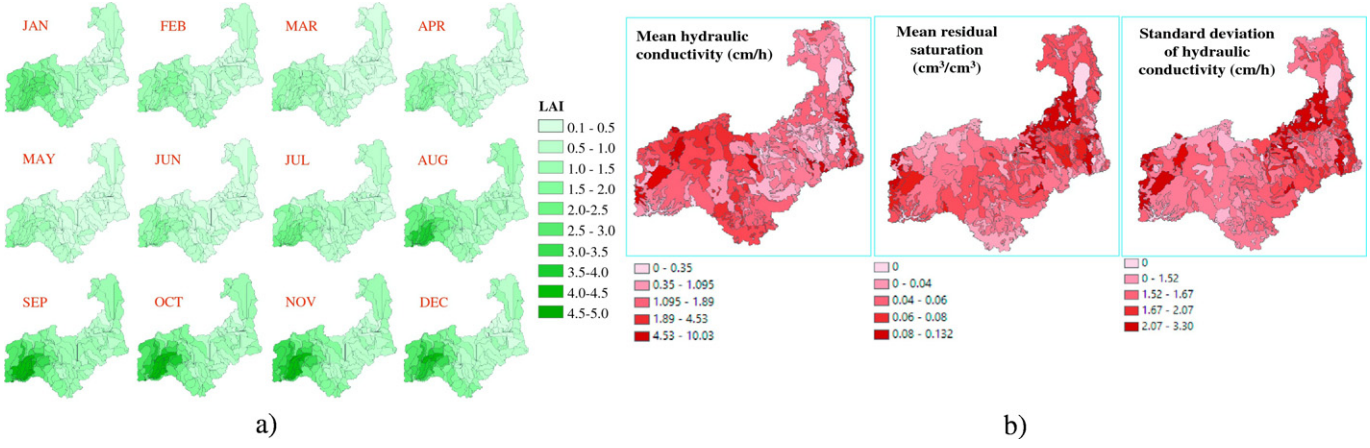

Fig. 3. a) Monthly average Leaf Area Index (LAI), and b) soil hydraulic parameters in the study watershed.

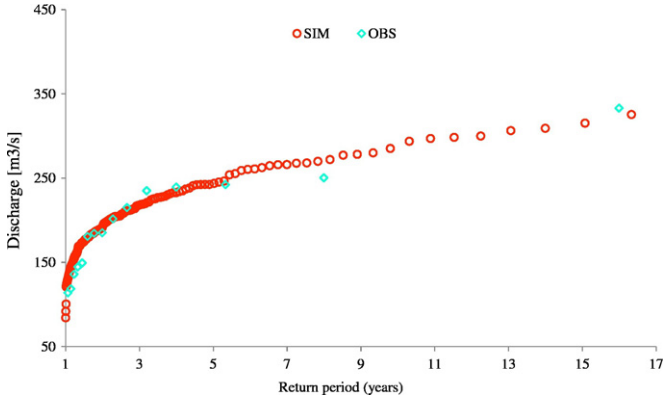

Fig. 4. Comparison of the annual mean flow as function of the return period between the model-simulations and corresponding observations at Shasta Dam's inflow station (2001–2015).

provided at hourly steps for the future (2016–2100) periods. The projected Shasta Dam inflow information was obtained from the WEHY-HCM- downscaled climate projections of the GCMs, ECHAM5 and CCSM3. These simulated dam inflows were compared with the water demand that were obtained from Trinh et al. (2016b). It is noted that there are thirteen individual climate projections. Thus WEHY-HCM is able to provide thirteen individual inflow projections to Shasta Dam.

A drought event is defined as an event during which streamflow is continuously below a specified level (Shiau and Shen, 2001). Yevjevich (1967) applied the "theory of runs" in determining the properties of hydrologic droughts, as illustrated in Fig. 5. Streamflow (Qt in Fig. 5) is considered as the water supply (inflow to Shasta Dam) in the present study. The level $Q_{0,t}$ (Fig. 5) is the water demand, which serves to divide the water supply series into above-water demand and below-water demand level sections, with drought events occurring in sections where the streamflow is continuously below the truncation level.

From the Fig. 5, one can also identify the drought duration and severity, the former being the period during which streamflow is continuously below the truncation level, while the latter being the cumulative deficit below the truncation level for the duration of a drought event. On the other hand, non-drought (surplus) duration and non-drought severity (cumulative surplus) are the time period and cumulative deviation above the truncation level during a water surplus event (Shiau and Shen, 2001).

In this analysis, surplus water is defined as the amount of water supply exceeding the water demand, while water deficit is defined as the amount of water supply that is unavailable to meet the water demand. For the estimation of the monthly water deficit or surplus, the specific month's Shasta Dam water demand is supposed to be subtracted from the corresponding Shasta Dam inflow. The residual of this operation is supposed to become that month's water deficit or surplus. For this study, the drought duration, D, is defined as the number of months for which the monthly deficit values are below zero, and the drought severity, S, is the cumulative sum of the monthly deficit for that particular drought event. The drought duration is the number of months per year when the anomaly is below zero. The drought intensity, I, is the ratio between the severity (S) and duration (D).

$$I = \frac{S}{D} \tag{1}$$

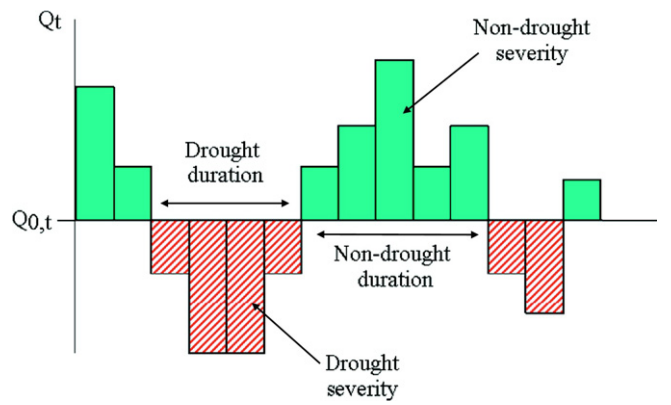

Fig. 5. Concept and definition of a drought event, drought duration, and drought severity.

4. Results and discussion of future drought conditions at Shasta Dam

It is difficult to adopt a specific GCM and a specific emissions scenario for the projection of the future climate because the future climate conditions are unknown and are evolving in time and space. One plausible approach to the projection of the future climate over Shasta Dam watershed is the development of an ensemble of projections, and then use the ensemble average of all individual projection realizations (13 realizations in this project) for the future climate projection with maximum and minimum bands. It is noted that the future drought analysis in this study is based on the assumption that each future projection is equally likely to occur.

Based on projected Shasta Dam annual inflows from the downscaling of thirteen GCMs climate projections, and annual water demand obtained from the previous study (Trinh et al., 2016b), a comparison between the future ensemble average inflow and water demand was made for Shasta Dam as shown in Fig. 6.

As seen from the Fig. 6, the blue bar represents the ensemble average of the 13 projections of the annual water supply (inflow to Shasta Dam), the green line represents the annual water demand, and the red bar with a band shows the maximum and minimum values from results of the 13 projections of the annual water supply at Shasta Dam. In order to compare the future drought conditions with the historical one, Fig. 7 shows the historical annual water supply which was reconstructed from the downscaling of NCEP historical reanalysis data (Trinh et al., 2016b), and the water demand which is the same as the one in Fig. 6 (Trinh et al., 2016b). From Fig. 7 one can clearly notice several drought years in which annual mean inflow does not meet annual water demand, such as the ones during 1955, 1976–1977, 1985 and 1987–1992. Among these, the drought years of 1976–1977 far exceeded in dryness the State of California's prior record of two year dry periods (DWR, 1978), while the period 1987–1992 was the longest historical

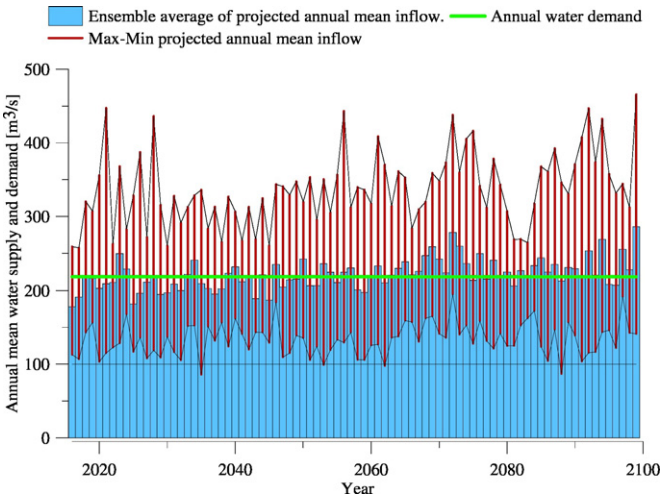

Fig. 6. Comparison between future ensemble average water supply and water demand at Shasta Dam.

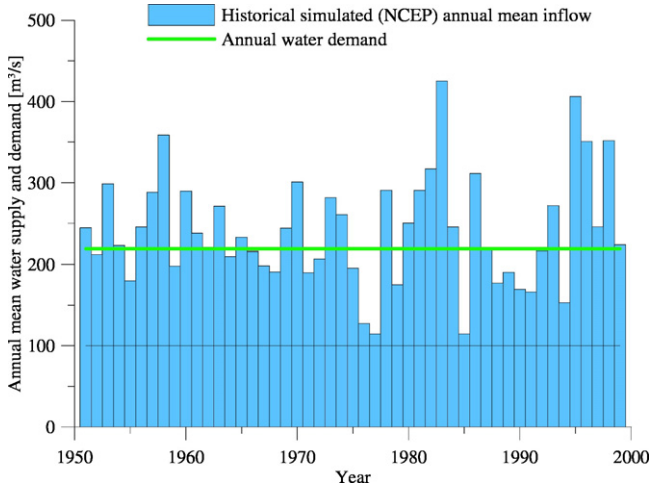

Fig. 7. Comparison between historical water supply and water demand at Shasta Dam.

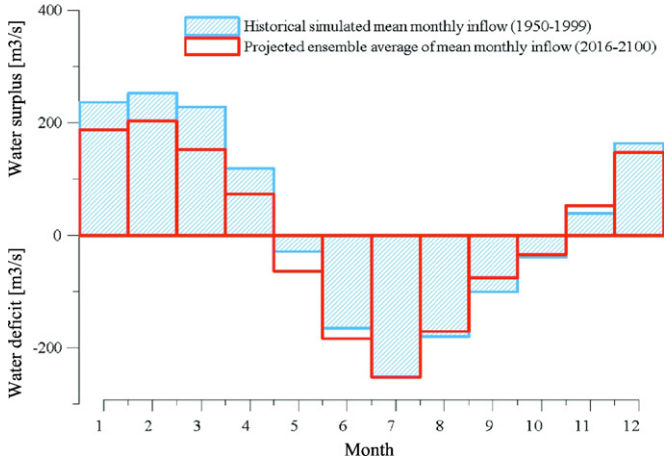

Fig. 9. Comparison of the monthly climatology of historical and the ensemble average of the future water surplus and deficit at Shasta Dam.

drought event at Shasta Dam. It is noted that none of the historical annual mean water supplies are below the level of 100 [m^3/s], while there are several future annual mean water supplies that are below the level of 100 [m^3/s], as can be seen in the minimum band. Based on this evaluation, one can infer that drought conditions could be more severe in the future.

In order to have an assessment with a different perspective on the drought events with respect to surplus and deficit which were defined in the previous Section, the monthly climatology was then examined for the future water surplus and deficit. Fig. 8 shows the average of the simulated monthly mean water surplus and deficit over the future period 2016–2100 for the 13 projections. Based on Fig. 8, it can be seen that there is no clear difference in water deficit among the future projections from May to October, but it can be clearly seen that water deficit is the largest in July, and the lowest in October in the all of projections.

The ensemble average of all future projections from ECHAM5 and CCSM3 GCMs was computed in terms of the mean monthly water surplus and deficit, and then it was compared with the corresponding historical data. As shown in Fig. 9, it may be inferred that the future droughts may be more extreme in May and June, while they may be less extreme in August and September when compared to historical periods. In addition, future surpluses are smaller from December to April when compared to historical periods.

To analyze the relationship between projected drought severity and duration for Shasta Dam during 21st century, Fig. 10 gives a scatter plot of the severity of the projected water deficit events versus their duration. The deficit durations can be roughly classified into two categories: events lasting up to 16 months, and events lasting between 16 and 24 months. The majority of events, approximately 95%, have durations less than or equal to 16 months, and approximately 5% have durations between 16 and 24 months. As can be seen from this figure, the longest drought event belongs to that based on the A1B2 scenario from ECHAM5 and *B*1 scenario from CCSM3 with 21 months. The second longest drought lasted for 20 months in A1B3 scenario from ECHAM5. Interestingly, the most severe simulated future drought event is not the longest duration event. In looking at the comparison of drought severity and duration between future and historical periods, it can be seen that the most severe simulated historical drought event (based on NCEP reanalysis climate data) occurred within 19 months, and it is the 1976–1977 drought event. Thus, it may be inferred that the future drought events may not only be more severe, but also may last longer. Together with more severe and longer drought events, the number of drought events also increases in the future. This inference is based on the histograms of water deficit intensities, shown in Fig. 11.

From this figure it can be clearly seen that the number of future drought events in the second half of the 21st century are more frequent than the number of the historical events with 60 events for the future and 53 events for the historical period. As shown in Fig. 11, the majority of future and historical drought events have intensities within 120–140 [m^3/s]/months with 17 events for future, and 13 events for the historical period.

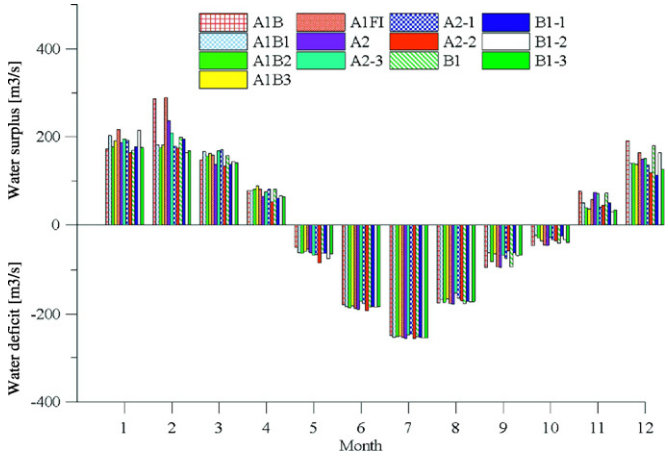

Fig. 8. Monthly water surplus and deficit for each future projection at Shasta Dam.

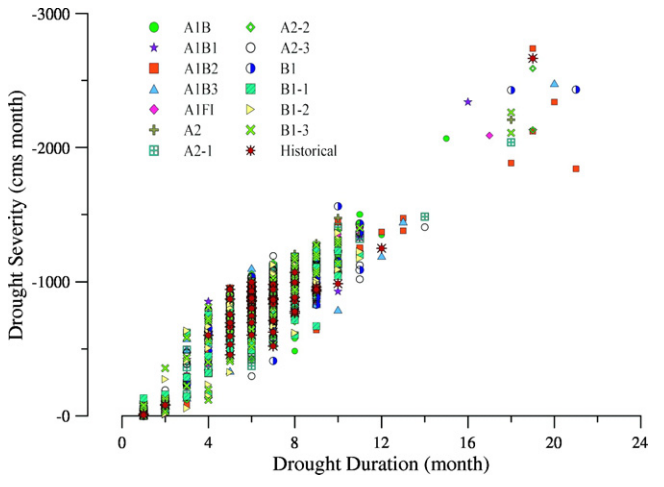

Fig. 10. Relationship between drought duration and severity at Shasta Dam during the 21st century.

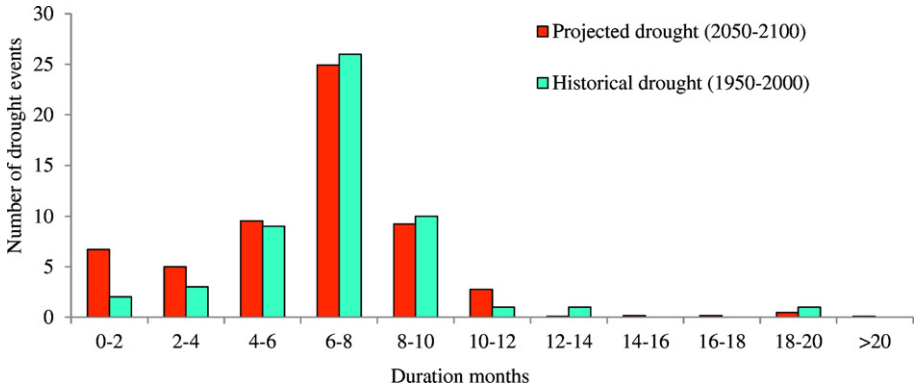

Fig. 11. Histogram of the historical and projected monthly drought intensities at Shasta Dam during the 21st century based on the ensemble average of all projections.

In order to analyze the change in drought regime from historical to future periods, the probabilistic structure of the projected drought conditions at Shasta Dam is presented by means of drought intensity as a function of the return period. The future return period was computed from an ensemble of thirteen individual drought intensity projections from 2016 to 2100, while the historical return period was computed from NCEP reanalysis climate data for 1950–2000. In this figure there is an increasing trend in drought intensity with the return period, independent of the time window. This result confirms that the future drought regime may be more severe than that of the historical period. It may also be noted that this study estimated the future drought conditions based on a large sample corresponding to 13 future climate projections. As such, the 100-year and 200-year return period droughts were estimated at Shasta Dam without resorting to any extrapolation of the frequency curve.

The findings of this study fundamentally agree with those of previous studies in other regions of California. Zhu et al. (2005) found that significant climate warming can decrease state water supply availabilities and increase water demand, leading to increased drought risk in California. Diffenbaugh et al. (2015) found that the increasing co-occurrence of dry years with warm years raises the drought severity and duration despite the trend of future precipitation.

This study proposes a methodology to examine future drought conditions over a selected watershed by means of a physically based Hydro-Climate Model. Although the methodology used in this study is computationally intensive, it was possible to account for the complicated nonlinearity of atmospheric and hydrologic processes corresponding to thirteen climate projections. The projected variables in this study can be used for the estimation of different drought categories including meteorological, agricultural, and hydrological droughts under a variety of drought indexes. Based on the large sample of projections, the proposed approach can estimate the drought properties of the 100-year and 200-year return periods without resorting to any extrapolation of the frequency curve. However, this study assumed water demand and the fundamental physical characteristics such as topography, land use/cover, vegetation, and hydraulic infrastructure unchanged through the future period. Water demand and those physical characteristics are expected to change in the future. In order to improve the reliability of the proposed approach, future studies should account for projected water demand at Shasta Dam and potential change in fundamental physical characteristics over Shasta Dam watershed.

5. Conclusions

This study attempts to project drought conditions at Shasta Dam during the 21st century through the projections of the durations, severities, and intensities of these droughts. Analyses of the projected droughts at Shasta Dam were performed based on the historical and the projected future water supply conditions of Shasta Dam, and the historical water demand from the Dam in order to assess the change in drought characteristics during the 21st century. Based upon the comparison of drought durations and severities between the future and historical periods, it can be concluded that future drought events would be more severe, and longer than historical ones. Future drought events can last up to 21 months, while the longest simulated historical drought event was 19 months during 1976–1977. In addition to increased severity and duration of drought events, the number of drought events also increases in the future. During the 2050–2100 period, 60 drought events were projected. There were 53 drought events during the 1950–2000 historical period. Drought events in the second half of the 21st century are more frequent than those in the second half of the 20th century. In addition, the future drought regime may have a more severe pattern when compared to its historical counterpart. This phenomenon can be discerned from the probabilistic structure of drought intensities in Fig. 12. Based on the

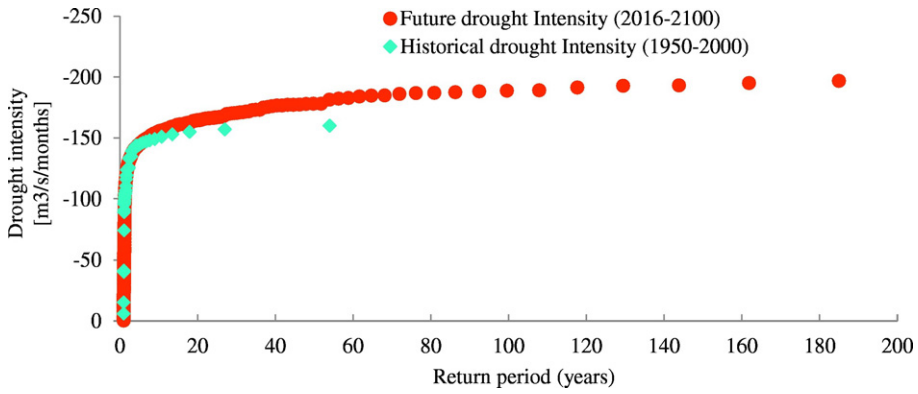

Fig. 12. Evolution of the drought intensity as function of return period during the second half of the 20th century and the end of 21st century.

large sample of thirteen projections, it is possible to perform a frequency analysis of the drought properties at Shasta Dam, and estimate the drought properties of the 100-year and 200-year return periods without resorting to any extrapolation of the frequency curve. In the future, it is possible to improve the reliability of the proposed approach. Projected land use and land cover of the study area and the future water demands that may evolve with time can be taken into account for a more reliable future drought analysis at Shasta Dam. In addition, a new approach for determining the greenhouse gases' (GHG) concentrations has evolved in recent years, and the range of GHG scenarios used in the latest IPCC assessment from 2013 (AR5) is referred to as Representative Concentration Pathways (RCP) scenarios. GCMs' global climate projections based on AR5 scenarios can be useful in refining the estimates of drought conditions in the future.

References

Adam, J.C., Hamlet, A.F., Lettenmaier, D.P., 2009. Implications of global climate change for snowmelt hydrology in the twenty-first century. Hydrol. Process. 23 (7), 962–972.

Anderson, M., Chen, Z., Kavvas, M., Yoon, J., 2007. Reconstructed historical atmospheric data by dynamical downscaling. J. Hydrol. Eng. 12 (2), 156–162.

Bonaccorso, B., Bordi, I., Cancelliere, A., Rossi, G., Sutera, A., 2003. Spatial variability of drought: an analysis of the SPI in Sicily. Water Resour. Manag. 17 (4), 273–296.

Cayan, D.R., et al., 2010. Future dryness in the southwest US and the hydrology of the early 21st century drought. Proc. Natl. Acad. Sci. 107 (50), 21271–21276.

Chen, Z., Kavvas, M., Fukami, K., Yoshitani, J., Matsuura, T., 2004a. Watershed environmental hydrology (WEHY) model: model application. J. Hydrol. Eng. 9 (6), 480–490.

Chen, Z., et al., 2004b. Geomorphologic and soil hydraulic parameters for Watershed Environmental Hydrology (WEHY) model. J. Hydrol. Eng. 9 (6), 465–479.

Collins, W.D., et al., 2006. The community climate system model version 3 (CCSM3). J. Clim. 19 (11), 2122–2143.

Cook, K.H., 2008. Climate science: the mysteries of Sahel droughts. Nat. Geosci. 1 (10), 647–648.

Council, A, 1997. Policy statement: meteorological drought. Bull. Am. Meteorol. Soc. 78, 847–849.

Daly, C., et al., 2008. Physiographically sensitive mapping of climatological temperature and precipitation across the conterminous United States. Int. J. Climatol. 28 (15), 2031–2064.

Diffenbaugh, N.S., Swain, D.L., Touma, D., 2015. Anthropogenic warming has increased drought risk in California. Proc. Natl. Acad. Sci. 112 (13), 3931–3936.

Dirmeyer, P.A., Brubaker, K.L., 1999. Contrasting evaporative moisture sources during the drought of 1988 and the flood of 1993. J. Geophys. Res. Atmos. 104 (D16), 19383–19397.

Dosio, A., Paruolo, P., 2011. Bias correction of the ENSEMBLES high-resolution climate change projections for use by impact models: evaluation on the present climate. J. Geophys. Res. Atmos. 116 (D16).

Dudhia, J., 1989. Numerical study of convection observed during the Winter Monsoon Experiment using a mesoscale two–dimensional model. J. Atmos. Sci. 46, 3077–3107.

Dudhia, Jimy, 1996. A Multi-layer Soil Temperature Model for MM5. The Sixth PSU/NCAR Mesoscale Model Users' Workshop.

Dunne, T., 1978. Field studies of hillslope flow processes. In: Kirkby, M.J. (Ed.), Hillslope Hydrology. Wiley, London, pp. 227–293 (Chapter 7).

Dutra, E., et al., 2013. The 2010–2011 drought in the Horn of Africa in ECMWF reanalysis and seasonal forecast products. Int. J. Climatol. 33 (7), 1720–1729.

DWR, 1978. The 1976–1977 California Drought, a Review, State of California, The Resources Agency.

DWR, 2013. Upper Sacramento, McCloud, and Lower Pit, Integrated Regional Water Management Plan, Regional Water Management Group.

Flato, Gregory, et al., 2013. Evaluation of climate models. In: climate change 2013: the physical science basis. Contribution of working group I to the fifth assessment report of the intergovernmental panel on climate change. Climate Change 2013 (5), 741–866.

Ghosh, S., Mujumdar, P., 2007. Nonparametric methods for modeling GCM and scenario uncertainty in drought assessment. Water Resour. Res. 43 (7).

Grell, G.A., 1995. A Description of the Fifth-Generation Penn State/NCAR Mesoscale Model (MM5), NCAR/TN-398 + STR. NCAR Technical Note.

Hawkins, E., Sutton, R., 2009. The potential to narrow uncertainty in regional climate predictions. Bull. Am. Meteorol. Soc. 90 (8), 1095.

Hollinger, S., Isard, S., Welford, M., 1993. A New Soil Moisture Drought Index for Predicting Crop Yields, Preprints, Eighth Conference on Applied Climatology. pp. 187–190.

Hong, S.Y., Pan, H.L., 1996. Nonlocal boundary layer vertical diffusion in a medium-range forecast model. Mon. Weather Rev. 124 (10), 2322–2339.

Horne, F.E., Kavvas, M.L., 1997. Physics of the spatially averaged snowmelt process. J. Hydrol. 191 (1), 179–207.

Jang, S., Kavvas, M., 2013. Downscaling global climate simulations to regional scales: statistical downscaling versus dynamical downscaling. J. Hydrol. Eng. 20 (1), A4014006.

Kain, John S., 2004. The Kain–Fritsch convective parameterization: an update. J. Appl. Meteorol. 43, 170–181.

Kalnay, E., et al., 1996. The NCEP/NCAR 40-year reanalysis project. Bull. Am. Meteorol. Soc. 77 (3), 437–471.

Kavvas, M., et al., 2004. Watershed environmental hydrology (WEHY) model based on upscaled conservation equations: hydrologic module. J. Hydrol. Eng. 9 (6), 450–464.

Kavvas, M., Kure, S., Chen, Z., Ohara, N., Jang, S., 2013. WEHY-HCM for modeling interactive atmospheric-hydrologic processes at watershed scale. I: model description. J. Hydrol. Eng. 18 (10), 1262–1271.

Keyantash, J.A., Dracup, J.A., 2004. An aggregate drought index: assessing drought severity based on fluctuations in the hydrologic cycle and surface water storage. Water Resour. Res. 40 (9).

Kirono, D., Kent, D., Hennessy, K., Mpelasoka, F., 2011. Characteristics of Australian droughts under enhanced greenhouse conditions: results from 14 global climate models. J. Arid Environ. 75 (6), 566–575.

Madadgar, S., Moradkhani, H., 2011. Drought analysis under climate change using copula. J. Hydrol. Eng. 18 (7), 746–759.

Maurer, E.P., 2007. Uncertainty in hydrologic impacts of climate change in the Sierra Nevada, California, under two emissions scenarios. Clim. Chang. 82 (3–4), 309–325.

Maurer, E.P., Duffy, P.B., 2005. Uncertainty in projections of streamflow changes due to climate change in California. Geophys. Res. Lett. 32 (3).

McKee, T.B., Doesken, N.J., Kleist, J., 1993. The relationship of drought frequency and duration to time scales. Proceedings of the 8th Conference on Applied Climatology. American Meteorological Society Boston, MA, pp. 179–183.

McKee, T., Doesken, N., Kleist, J., 1995. Drought Monitoring with Multiple Time Scales, Proceedings of the. 9th Conference on Applied Climatology. American Meteorological Society Dallas, Boston, MA, Pp, pp. 233–236.

Milly, P., et al., 2007. Stationarity is dead. Ground Water News Views 4 (1), 6–8.

Mishra, V., Cherkauer, K.A., Shukla, S., 2010. Assessment of drought due to historic climate variability and projected future climate change in the midwestern United States. J. Hydrometeorol. 11 (1), 46–68.

Nalbantis, I., 2008. Evaluation of a hydrological drought index. Eur. Water 23 (24), 67–77.

Ohara, N., Kavvas, M., 2006. Field observations and numerical model experiments for the snowmelt process at a field site. Adv. Water Resour. 29 (2), 194–211.

Ohara, N., Chen, Z., Kavvas, M., Fukami, K., Inomata, H., 2010. Reconstruction of historical atmospheric data by a hydroclimate model for the Mekong River basin. J. Hydrol. Eng. 16 (12), 1030–1039.

Ohara, N., Kavvas, M., Anderson, M., Richard Chen, Z., Yoon, J., 2011. Water balance study for the Tigris-Euphrates river basin. J. Hydrol. Eng. 16 (12), 1071–1082.

Palmer, W.C., 1965. Meteorological Drought. 30. US Department of Commerce, Weather Bureau, Washington, DC.

Palmer, W.C., 1968. Keeping Track of Crop Moisture Conditions, Nationwide: The New Crop Moisture Index.

Pereira, L.S., Cordery, I., Iacovides, I., 2002. Coping with water scarcity. Technical Documents in Hydrology 58. Unesco, Paris.

Prudhomme, C., et al., 2014. Hydrological droughts in the 21st century, hotspots and uncertainties from a global multimodel ensemble experiment. Proc. Natl. Acad. Sci. 111 (9), 3262–3267.

Raziei, T., Bordi, I., Pereira, L.S., 2011. An application of GPCC and NCEP/NCAR datasets for drought variability analysis in Iran. Water Resour. Manag. 25 (4), 1075–1086.

Reisner, J., Rasmussen, R.M., Bruintjes, R.T., 1998. Explicit forecasting of supercooled liquid water in winter storms using the MM5 mesoscale model. Q. J. R. Meteorol. Soc. 124, 1071–1107.

Roeckner, E., et al., 2003. The Atmospheric General Circulation Model ECHAM5. PART I: Model Description, Report 349. Max Planck Institute for Meteorology, Hamburg, Germany.

Rossi, G., Vega, T., Bonaccorso, B., 2007. Methods and Tools for Drought Analysis and Management. 62. Springer Science & Business Media.

Shafer, B., Dezman, L., 1982. Development of a Surface Water Supply Index (SWSI) to Assess the Severity of Drought Conditions in Snowpack Runoff Areas, Proceedings of the Western Snow Conference. Colorado State University, Fort Collins, CO, pp. 164–175.

Sheffield, J., Goteti, G., Wen, F., Wood, E.F., 2004. A simulated soil moisture based drought analysis for the United States. J. Geophys. Res. Atmos. 109 (D24).

Shiau, J.-T., Shen, H.W., 2001. Recurrence analysis of hydrologic droughts of differing severity. J. Water Resour. Plan. Manag. 127 (1), 30–40.

Shukla, S., Wood, A.W., 2008. Use of a standardized runoff index for characterizing hydrologic drought. Geophys. Res. Lett. 35 (2).

Teutschbein, C., Seibert, J., 2012. Bias correction of regional climate model simulations for hydrological climate-change impact studies: review and evaluation of different methods. J. Hydrol. 456, 12–29.

Trinh, T., et al., 2016a. New methodology to develop future flood frequency under changing climate by means of physically based numerical atmospheric-hydrologic modeling. J. Hydrol. Eng. 21 (4), 04016001.

Trinh, T., et al., 2016b. Reconstruction of historical inflows into and water supply from Shasta Dam by coupling physically based hydroclimate model with reservoir operation model. J. Hydrol. Eng. 04016029.

Uppala, S.M., Kållberg, P.W., Simmons, A.J., Andrae, U., Bechtold, V.D., Fiorino, M., ... Li, X., 2005. The ERA-40 re-analysis. Q. J. R. Meteorol. Soc. 131 (612), 2961–3012.

Vogel, R.M., 1987. Reliability indices for water supply systems. J. Water Resour. Plan. Manag. 113 (4), 563–579.

Xin, X., Yu, R., Zhou, T., Wang, B., 2006. Drought in late spring of South China in recent decades. J. Clim. 19 (13), 3197–3206.

Xu, C.-y., 1999. From GCMs to river flow: a review of downscaling methods and hydrologic modelling approaches. Prog. Phys. Geogr. 23 (2), 229–249.

Yevjevich, V.M., 1967. An objective approach to definitions and investigations of continental hydrologic droughts. Hydrol. Pap. 23 (Colorado State University).

Zhu, T., Jenkins, M.W., Lund, J.R., 2005. Estimated Impacts of Climate Warming on California Water Availability Under Twelve Future Climate Scenarios. 1.